J. Fluid Mech. (1967), *vol.* 30, *part* 3, *pp.* 577–600
Printed in Great Britain

Finite amplitude convection cells

By J. L. ROBINSON

Mathematics Department, Imperial College, London†

(Received 12 November 1966 and in revised form 21 June 1967)

In this paper we consider two-dimensional steady cellular motion in a fluid heated from below at large Rayleigh number and Prandtl number of order unity. This is a boundary-layer problem and has been considered by Weinbaum (1964) for the case of rigid boundaries and circular cross-section. Here we consider cells of rectangular cross-section with three sets of velocity boundary conditions: all boundaries free, rigid horizontal boundaries and free vertical boundaries (referred to here as periodic rigid boundary conditions), and all boundaries rigid; the vertical boundaries of the cells are insulated. It is shown that the geometry of the cell cross-section is important, such steady motion being not possible in the case of free boundaries and circular cross-section; also that the dependence of the variables of the problem on the Rayleigh number is determined by the balances in the vertical boundary layers.

We assume only those boundary layers necessary to satisfy the boundary conditions and obtain a Nusselt number dependence $N \sim R^{\frac{1}{3}}$ for free vertical boundaries. For the periodic rigid case, Pillow (1952) has assumed that the buoyancy torque is balanced by the shear stress on the horizontal boundaries; this is equivalent to assuming velocity boundary layers beside the vertical boundaries (rather than the vorticity boundary layers demanded by the boundary conditions) and leads to a Nusselt number dependence $N \sim R^{\frac{1}{4}}$. If it is assumed that the flow will adjust itself to give the maximum heat flux possible the two models are found to be appropriate for different ranges of the Rayleigh number and there is good agreement with experiment.

An error in the application of Rayleigh's method in this paper is noted and the correct method for carrying the boundary-layer solutions round the corners is given. Estimates of the Nusselt numbers for the various boundary conditions are obtained, and these are compared with the computed results of Fromm (1965). The relevance of the present work to the theory of turbulent convection is discussed and it is suggested that neglect of the momentum convection term, as in the mean field equations, leads to a decrease in the heat flux at very high Rayleigh numbers. A physical argument is given to derive Gill's model for convection in a vertical slot from the Batchelor model, which is appropriate in the present work.

1. Introduction

The onset of motion in a fluid heated from below is now well understood. Above a critical Rayleigh number steady convection cells are set up, and the motion in the range just above this critical Rayligh number has been studied by many authors (see, for example, the review article by Segel (1966)).

† Now at the Department of Mathematics, University of Bristol.

If the Rayleigh number is further increased, time-dependent motion and then fully developed turbulence set in. It is considered to be of value to study steady convection at large Rayleigh numbers, both for a better understanding of the cellular motion, and, hopefully, to follow the breakdown of such motion.

Two-dimensional cells for Prandtl number of order unity are studied here. The theoretical results may then be compared with the values computed by Fromm (1965).

The equations of the Boussinesq approximation are used (this problem of convection between parallel plates has been well stated in many references, for example Chandrasekhar (1961)). The equations are

$$\left(\frac{\partial}{\partial t}+\mathbf{v}.\boldsymbol{\nabla}\right)T = \kappa\nabla^2 T, \tag{1}$$

$$\left(\frac{\partial}{\partial t}+\mathbf{v}.\boldsymbol{\nabla}\right)\mathbf{v} = -\boldsymbol{\nabla}\left(\frac{p}{\rho_0}\right)+\nu\nabla^2\mathbf{v}+g\alpha(T-T_0)\hat{k}, \tag{2}$$

$$\boldsymbol{\nabla}.\mathbf{v} = 0, \tag{3}$$

where $\mathbf{v}$ = velocity, T = temperature, T_0 = mean temperature, ν = kinematic viscosity (constant), κ = thermometric conductivity (constant), α = coefficient of thermal expansion, p = pressure $-\rho_0 gz$, ρ_0 = density. The co-ordinates are z (vertical) and x in the plane of the two-dimensional cell; $\hat{\imath}$ denotes a unit vector in the $+x$ direction, $\hat{\jmath}$ a unit vector in the $+y$ direction and $\hat{k}$ a unit vector in the $+z$ direction.

We non-dimensionalize as follows:

$$\mathbf{r} = d\mathbf{r}', \quad t = \frac{d^2}{\kappa}t', \quad v = \frac{\kappa}{d}v', \quad T = T_0+\Delta T\theta, \quad p = \frac{\kappa\nu\rho_0}{d^2}p',$$

where the temperature difference between the plates is $2\Delta T$, the separation of the plates is d.

A stream function is introduced so the velocity is given by $\mathbf{v} = \boldsymbol{\nabla}\times(\psi\hat{\jmath})$. For steady motion, dropping the primes, we find

$$-J(\psi,\theta) = (\mathbf{v}.\boldsymbol{\nabla})\theta = \nabla^2\theta, \tag{4}$$

$$\frac{1}{\sigma}(\mathbf{v}.\boldsymbol{\nabla})\mathbf{v} = -\boldsymbol{\nabla}p+\nabla^2\mathbf{v}+R\theta\hat{k}, \tag{5}$$

and, eliminating the pressure from (5),

$$\nabla^2\eta+(1/\sigma)J(\psi,\eta) = R\theta_x, \tag{6}$$

where J is the Jacobian,

$$J(a,b) = \frac{\partial a}{\partial x}\frac{\partial b}{\partial z}-\frac{\partial a}{\partial z}\frac{\partial b}{\partial x};$$

η is the vorticity $\eta = -\nabla^2\psi$; R is the Rayleigh number $R = g\alpha\Delta T d^3/\kappa\nu$; σ is the Prandtl number $\sigma = \nu/\kappa$.

It should be noted that the final non-dimensionalization for the velocity, giving $v_{\text{scaled}} \sim 1$, is not determined by the free or rigid boundary conditions alone; for large Rayleigh numbers we take $v \sim R^b$ in the above equations and determine b by the balances in the vertical boundary layers.

We consider here fluids within the regions $0 \leqslant z \leqslant 1$, $0 \leqslant x \leqslant L$, for three sets of velocity boundary conditions. The temperature boundary conditions are for all cases

$$\theta = \begin{matrix} -1 \\ +1 \end{matrix} \quad \text{on} \quad z = \begin{matrix} 1 \\ 0 \end{matrix}, \quad \theta_x = 0 \quad \text{on} \quad x = 0, L.$$

Free case: free boundary conditions at the horizontal boundaries (zero tangential viscous stress), periodic vertical boundary conditions; that is, free vertical boundaries from the asymmetry of the single cell problem—see Fromm (1965).

The boundary conditions are: $\psi = \eta = 0$ on all boundaries. It should be noted that for free boundary conditions and circular cross-section the only non-zero torque is that due to the buoyancy forces and steady cellular motion is therefore not possible (for any temperature boundary conditions). For rectangular cross-section the pressure and normal viscous stress give rise to a balancing torque and this problem is solved below in good agreement with the calculations of Fromm (1965). The geometry of the cell cross-section is thus seen to be of importance in this problem.

Rigid case: all boundaries rigid (zero velocity). The boundary conditions are: $\psi = 0$ on all boundaries; $\partial\psi/\partial x = 0$ on $x = 0, L$; $\partial\psi/\partial z = 0$ on $z = 0, 1$.

Periodic rigid case: rigid horizontal boundaries, periodic vertical boundary conditions. The boundary conditions are: $\psi = 0$ on all boundaries; $\partial\psi/\partial z = 0$ on $z = 0, 1$; $\eta = 0$ on $x = 0, L$.

For this set of boundary conditions and $\sigma = 1$ the problem of two-dimensional cells may be shown to be equivalent to that of steady axisymmetric cellular motion between two rigid rotating cylinders provided that the following relations hold:

$$\text{(i)} \quad \frac{\delta r}{r} \ll 1,$$

$$\text{(ii)} \quad \frac{\delta\Omega}{\Omega} \ll 1,$$

$$\text{(iii)} \quad T = -2\frac{\Omega^2(\delta r)^4}{\nu^2}\left(1 + \frac{r\,\delta\Omega}{2\delta r\,\Omega}\right),$$

where Ω_1 is the angular velocity of the inner cylinder, Ω_2 is the angular velocity of the outer cylinder, $\delta\Omega = \Omega_2 - \Omega_1$ and Ω is the average angular velocity of the cylinders; $\delta r = r_2 - r_1$ and r is the average radius of the cylinders; T is the Taylor number and is equivalent to the Rayleigh number in the present problem. This equivalence is discussed in Chandrasekhar (1961) for the linear stability problem.

2. Formulation

2.1. *Balances*

It is assumed that a boundary-layer solution exists and that the streamlines in each cell are closed. The variables are expanded in asymptotic series of interior and boundary-layer functions,

$$\psi = R^b\varphi_0(x,z) + R^{b-ma}\sum_{i=1}^{2}\varphi_{BL}^{(i)}(\xi,z) + R^{b-m'a'}\sum_{i=3}^{4}\varphi_{BL}^{(i)}(x,\zeta) + R^{b-ma}\varphi_1^{(a)}(x,z) + R^{b-m'a'}\varphi_1^{(b)}(x,z) + \ldots,$$

$$\theta = \theta_0(x,z) + \sum_{i=1}^{4}\theta_{BL}^{(i)} + \ldots,$$

where $i = 1, 2$ denote boundary-layer solutions in the vertical boundary layers, $i = 3, 4$ denote boundary-layer solutions in the horizontal boundaries. In later discussion we disregard the superscripts.

$\xi = R^{+a}x$ is a boundary-layer co-ordinate for a vertical boundary layer and $\zeta = R^{+a'}z$ is a boundary-layer co-ordinate for a horizontal boundary layer.

φ_0 is chosen to satisfy the boundary conditions $\varphi_0 = 0$ on all boundaries; the boundary-layer stream functions are introduced to satisfy the boundary conditions $\partial\psi/\partial n = 0$ (rigid boundaries) or $\partial^2\psi/\partial n^2 = 0$ (free boundaries) to order R^b, where n is the co-ordinate perpendicular to the boundary; the interior streamfunctions $\varphi_1^{(a)}$ and $\varphi_1^{(b)}$ are introduced so that $\psi = 0$ on all boundaries to order $\max(R^{b-ma}, R^{b-m'a'})$; further boundary-layer streamfunctions must then be introduced, and so on.

The constants b, a, a', m, m' will be determined later for the three sets of boundary conditions.

The driving force for the motion is the buoyancy which appears in (6) as $R\theta_x$. As this is greatest in the vertical boundary layers we require that the following balances hold in those regions.

(a) From equation (4) $J(\psi, \theta) \sim \nabla^2\theta$ within the boundary layer, i.e.

$$R^b = R^{2a}, \quad b = 2a \tag{7}$$

(provided the interior velocity is of importance in this layer; this is so for all cases considered here).

(b) From equation (6) $R\theta_x \sim \nabla^2\eta_{BL}$ or $R\theta_x \sim J(\psi, \eta_{BL})$ ($\sigma \sim 1$ here); i.e. $R^{1+a} = R^{b-ma+4a}$ or $R^{1+a} = R^{2b-ma+2a}$ (where $\eta_{BL} = -R^{b-ma}\nabla^2\varphi_{BL}$). Since $b = 2a$ these conditions are equivalent and all three terms are of importance in the boundary layer

$$(5-m)a = 1. \tag{8}$$

(c) The remaining balance is derived from the velocity boundary conditions on the vertical boundaries.

Free boundary conditions

$$\frac{\partial^2\psi}{dx^2} = 0; \quad \text{i.e.} \quad R^b\frac{\partial^2\varphi_0}{\partial x^2} + R^{b-ma+2a}\frac{\partial^2\varphi_{BL}}{\partial\xi^2} = 0, \quad m = 2. \tag{9}$$

From (7), (8), (9) we obtain $a = \frac{1}{3}, b = \frac{2}{3}$. Since heat flux $\sim$ velocity $\times$ temperature $\times$ horizontal extent $\sim R^{\frac{1}{3}}$, the Nusselt number $N \sim R^{\frac{1}{3}}$.

Rigid boundary conditions

$$\frac{\partial\psi}{\partial x} = 0; \quad \text{i.e.} \quad R^b\frac{\partial\varphi_0}{\partial x} + R^{b-ma+a}\frac{\partial\varphi_{BL}}{\partial\xi} = 0, \quad m = 1. \tag{10}$$

From (7), (8), (10) we obtain $a = \frac{1}{4}, b = \frac{1}{2}$.

$$\text{Heat flux} \sim R^{\frac{1}{4}},$$

$$N \sim R^{\frac{1}{4}}.$$

In order to provide the necessary conduction of heat through the horizontal boundaries we require (convection in vertical boundary layers) $\sim R^a \sim$ (conduction through horizontal boundaries) $= -\int(\partial\theta/\partial x)\,dz \sim R^{a'}$. Therefore $a' = a$;

the same balances then hold except that in all cases the buoyancy term does not appear in the highest-order horizontal boundary-layer equations. The scaling constants are then

$$\begin{aligned}
&\text{rigid case:} && b = \tfrac{1}{2}, \quad a = a' = \tfrac{1}{4}, \quad m = m' = 1;\\
&\text{free case:} && b = \tfrac{2}{3}, \quad a = a' = \tfrac{1}{3}, \quad m = m' = 2;\\
&\text{periodic rigid case:} && b = \tfrac{2}{3}, \quad a = a' = \tfrac{1}{3}, \quad m = 1, \quad m' = 2.
\end{aligned}$$

The above agrees with the result $N \sim R^{\frac{1}{4}}$ of Weinbaum (1964) for rigid boundary conditions and cylindrical geometry. In that paper, the result of the Nusselt number calculation is compared (p. 423) with heat transfer between two horizontal plates. The discussion given later in this paper indicates that below $R \approx 4 \times 10^5$ the heat flow predicted by the model with rigid boundary conditions should be a lower bound for the observed heat flux. Weinbaum has computed the heat flux for a Rayleigh number with the radius of the cylinder as the length scale and a temperature scale of half the maximum temperature difference. It is suggested that we should compare the heat flux for two plates separated by a distance d and with a temperature difference ΔT with the heat flux for a cylinder of diameter d and maximum temperature difference ΔT. If the Rayleigh number, R, has the latter length and temperature scales we find $N = 0{\cdot}118R^{\frac{1}{4}}$ (modified Oseen), which is about one-half of the value observed experimentally for flow between flat plates in the relevant range of Rayleigh number.

The balance for rigid boundary conditions also holds if we postulate velocity boundary layers near the vertical boundaries for free vertical boundary conditions. The result $N \sim R^{\frac{1}{4}}$ has been obtained by Pillow (1952) for the periodic rigid case using the equivalent assumption that the buoyancy torque is balanced by the moment of the shear stresses on the horizontal boundaries. In the present model, where we find $N \sim R^{\frac{1}{3}}$ for the periodic rigid case, the viscous torque is balanced by the second-order pressure. This may be shown as follows. (These torques are of order R; the buoyancy torque is of order $R^{\frac{2}{3}}$.)

In the horizontal boundary layers the highest-order velocity equation is

$$\frac{1}{\sigma}\left\{(u_0+u_{BL})\frac{\partial u_{BL}}{\partial x}+u_{BL}\frac{\partial u_0}{\partial x}\left(\frac{\partial v_0}{\partial z}\zeta+v_{BL}+v_1\right)\frac{\partial u_{BL}}{\partial \zeta}\right\} = \frac{\partial^2 u_{BL}}{\partial \zeta^2}, \tag{11}$$

where u_{BL}, v_{BL} are the boundary-layer velocities in the x, z directions, v_1 is the next-order interior velocity in the z direction. Integrating this equation over (x, ζ) space and making use of the boundary conditions

$$(u_0+u_{BL} = v_{BL}+v_1 = 0 \quad \text{on} \quad \zeta = 0, \quad u_{BL}, v_{BL} \to 0 \quad \text{as} \quad \zeta \to 0)$$

gives

$$-\int_0^L \frac{\partial u_{BL}}{\partial \zeta}(\zeta = 0)dx = +\frac{1}{\sigma}\int_0^L u_0 v_{BL}(\zeta = 0)\,dx.$$

The viscous drag is therefore balanced in this boundary-layer problem by a convection of momentum across the boundaries. The next-order interior flow must balance the normal boundary-layer velocities ($v_1 + v_{BL} = 0$ on the horizontal boundaries). There will therefore be momentum convection forces opposite to

those above acting on each horizontal boundary in the next-order interior problem. The interior balance is

$$\frac{1}{\sigma}\{(\mathbf{v}_0.\nabla)\mathbf{v}_1+(\mathbf{v}_1.\nabla)\mathbf{v}_0\} = -\nabla p_1,$$

and, since this balance holds throughout the fluid, the momentum torque will be balanced by a pressure torque. Thus the highest-order viscous drag gives rise to a torque which is balanced by the second-order interior pressure.

A criterion for choosing between the two models is discussed later in this paper.

2.2. *Interior solutions*

Here we introduce two assumptions basic to this cellular model; first that the interior streamlines are closed, and second that the interior velocity is non-zero. The assumptions are found to be consistent in this problem, but not for the case of side-to-side heating (a discussion of the latter problem is given later in this paper).

In the present scaling the interior streamfunction is of order $R^{\frac{2}{3}}$ for free vertical boundaries and of order $R^{\frac{1}{2}}$ for rigid vertical boundaries. The highest-order temperature equation (4) thus is in the interior

$$J(\varphi_0, \theta_0) = 0. \tag{12}$$

This gives $\theta_0 = \theta_0(\varphi_0)$; that is, θ_0 is constant along streamlines, which are closed. Since θ_0 is antisymmetric, this requires that $\theta_0 = 0$. It is easily shown that this argument carries through for the lower-order interior temperature terms and thus $\theta \equiv 0$ in the interior.

For both sets of vertical boundary conditions we have $J(\psi, \nabla^2\psi) \gg \nabla^4\psi$ in the interior, and thus $J(\varphi_0, \nabla^2\varphi_0) = 0$ from (6). That is,

$$\nabla^2\varphi_0 = G(\varphi_0). \tag{13}$$

In the interior we have steady laminar flow with closed streamlines and no external force field. For such a flow Batchelor (1956) has shown that around any closed streamline lying entirely within the core region

$$\oint(\nabla\times\boldsymbol{\eta}).\mathbf{ds} = 0, \quad \text{where } \boldsymbol{\eta} \text{ is the vorticity;}$$

i.e.
$$\oint(\nabla\times\nabla^2\varphi_0\hat{j}).\mathbf{ds} = G'(\varphi_0)\oint(\nabla\times\varphi_0\hat{j}).\mathbf{ds}$$
$$= G'(\varphi_0)\oint\mathbf{v}_0.\mathbf{ds}$$
$$= 0.$$

Since the circulation, $\oint\mathbf{v}_0.\mathbf{ds}$, is taken to be non-zero for this problem,

$$G(\varphi_0) = \nabla^2\varphi_0 = -\omega_0, \text{ a constant.} \tag{14}$$

Equation (14) may be solved satisfying the boundary condition $\varphi_0 = 0$ on all boundaries. Boundary-layer solutions must be introduced in order to satisfy the remaining boundary conditions; and this is consistent with the original assumption of this work.

2.3. *Treatment of the corners*

Pillow (1952) developed a crude approximation using a modification of Rayleigh's method for the flat plate boundary to obtain an estimate of the heat transfer in the periodic rigid case. In these calculations, on p. 25, we find the following remark concerning a vertical boundary layer: 'In this range of t there is no heat conduction across the boundary AB, so that

$$\int_0^\infty T(n.t)\,dn = \int_0^\infty T(n,0)\,dn \quad (-\tfrac{1}{2} < t < 0).'$$

(Here t is a time-like variable

$$t = \frac{1}{\mu}\int_0^s \frac{ds}{U(s)}, \quad \mu = \int_{-2}^{+2} \frac{ds}{U(s)}, \quad U(s) = w(t);$$

U is the velocity parallel to the boundary; s is a co-ordinate along the boundary.)

Since there is no heat conduction across this boundary, the *heat flux* in this boundary layer must be constant. That is,

$$w(t)\int_0^\infty T(n,t)\,dn = \text{constant} \quad (-\tfrac{1}{2} < t < 0),$$

where $w(t)$ varies in this region and $w(0) = 0$. Thus the above conclusion is incorrect and the theory breaks down at this point; the flow must spread out *in order of magnitude*, in order to transport the heat flux round each corner.

Once the flow has spread out, the conduction and creation terms in (4), (6) decrease in order of magnitude and thus in the corner regions we have

$$\left.\begin{aligned} J(\varphi_0, \theta_{BL}) &= 0, \\ J(\varphi_0, \eta_{BL}) &= 0; \end{aligned}\right\} \tag{15}$$

that is the boundary-layer temperature and vorticity are convected unchanged through this region, until they impinge on the next boundary-layer region.

3. Calculations

In order to solve this problem we must find a solution which satisfies the periodicity requirement; that is, the initial profile chosen for temperature or boundary-layer streamfunction must be matched by the solution after it has been followed around one circuit of the cell.

The calculations have been formulated in terms of the unknowns ω_0 and A, where $R^b\omega_0$ is the interior vorticity and R^aA is the heat flux convected along each vertical boundary layer (thus $2R^aA$ is the heat conducted across each horizontal boundary).

We obtain first the interior streamfunction and the temperature solution (with the Oseen approximation) and then find the solutions for the stream function boundary layers separately for the three sets of boundary conditions. When the heat conducted across the horizontal boundaries has been set equal to $2R^aA$ and the condition for the existence of a periodic boundary-layer stream function is known we have two equations from which we can find the two unknowns, A and w_0.

The interior streamfunction problem is specified by equation (14), $\nabla^2\varphi_0 = -\omega_0$, with boundary conditions $\varphi_0 = 0$ on all boundaries. The solution is:

$$\varphi_0(x,z) = -2\omega_0 \sum_1^\infty \frac{1-(-1)^n}{(n\pi)^3 \sinh n\pi L} \sin n\pi z \{\sinh n\pi x + \sinh n\pi(L-x) - \sinh n\pi L\}. \tag{16}$$

Each boundary layer is divided into three regions where (i) the flow is impinging on the boundary (figure 2, (*d*), (*h*)), (ii) the flow is parallel to the boundary ((*e*), (*a*)) and (iii) the flow is away from the boundary ((*f*), (*b*)); (*g*), (*c*) are small corner regions. The regions are defined by the lengths $x_1 = \mathscr{H}/B$ in the horizontal boundary layers, $z_1 = \alpha/B$ in the vertical boundary layers where $\mathscr{H}$, α, B are defined by the velocity approximations stated below and illustrated in figure 1.

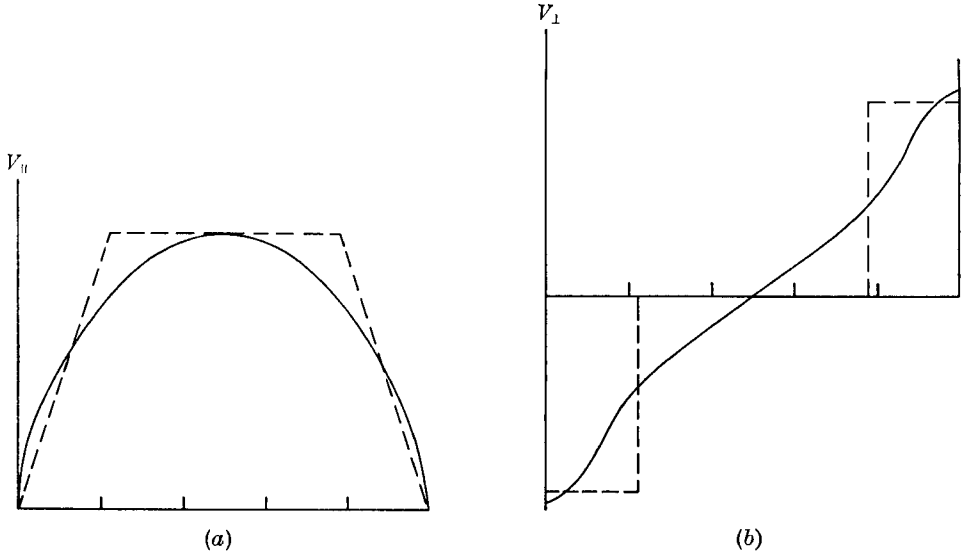

FIGURE 1. Interior velocity (*a*) parallel to the boundary, (*b*) perpendicular to the boundary with the approximations used.

The approximation used in the end regions of each boundary layer will be illustrated by considering the horizontal boundary-layer sub-region near $x = 0$. In this region the velocities will be approximated by

$$\text{vertical velocity} \approx -B\omega_0 \zeta R^{b-a},$$

$$\text{horizontal velocity} \approx +B\omega_0 x R^b$$

(ζ is the boundary-layer co-ordinate, $\zeta = R^a z$). B is obtained by taking the first N terms in the series expansion for the vertical velocity and using the approximation $\sin n\pi z \approx n\pi z$.

Then

$$B = l2\omega_0 \sum_1^N \frac{1-(-1)^n}{n\pi} \frac{\cosh n\pi L - 1}{\sinh n\pi L}. \tag{17}$$

The parameter l is introduced so that the dependence of the results on this approximation may be studied by computation (N is taken to be 5 in these computations).

In each mid-region the flow is approximately parallel to the boundary. In the lower horizontal boundary

$$\text{horizontal velocity} \approx \frac{\partial \varphi_0}{\partial z}\left(\frac{L}{2}, 0\right) R^b,$$

$$\approx \mathscr{H}\omega_0 R^b,$$

where
$$\mathscr{H} = 2\sum_1^N \frac{1-(-1)^n}{(n\pi)^2 \sinh n\pi L}\left\{\sinh n\pi L - 2\sinh\frac{n\pi L}{2}\right\}. \tag{18}$$

On the left ($x = 0$) vertical boundary

$$\text{vertical velocity} \approx -\frac{\partial \varphi_0}{\partial z}(0, \tfrac{1}{2}) \approx -\alpha w_0 R^b,$$

where
$$\alpha = 2\sum_1^N \frac{1-(-1)^n}{(n\pi)^2 \sinh n\pi L}(-1)^{(\frac{1}{2}n-1)}\{\cosh n\pi L - 1\}. \tag{19}$$

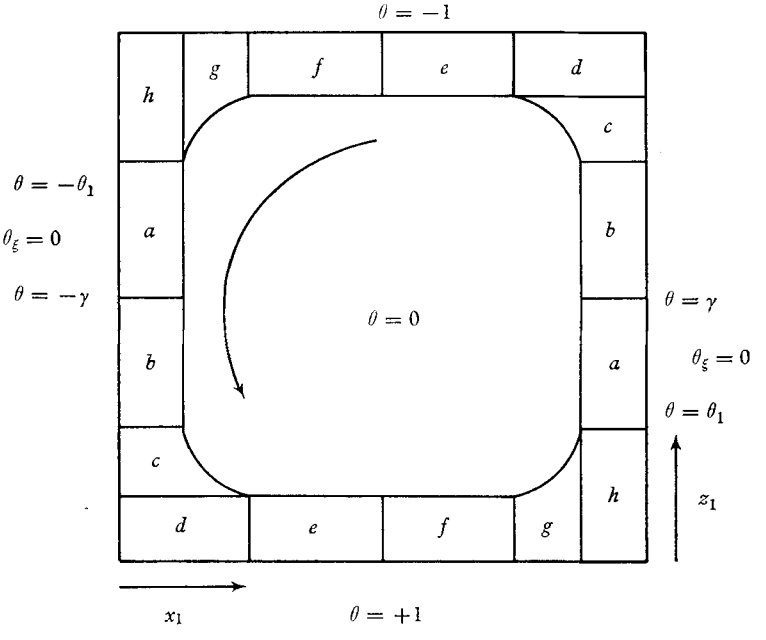

FIGURE 2. Boundary-layer regions.

An initial profile is chosen and solutions are obtained for each successive region, following the direction of the flow; the output from each region becoming the input to the following region. These solutions must then satisfy the periodicity requirement that the initial profile chosen be matched by the solution after it has been followed around one circuit of the cell.

The method used for turning the corners is as follows. The incoming profile is known—for example the limit of the solution in region b as $z \to 0$ is the input to the corner region c (see figure 2). This profile is carried through the corner along the (approximate) streamlines xz = constant and is then taken to be incident on

the region d at a distance of $R^{-a}\mathscr{L}$ (i.e. $\zeta = \mathscr{L}$) from the x-axis. Once the solution to this problem has been found $\mathscr{L}$ is taken to infinity.

In rigid-boundary boundary layers the modified Oseen approximation as described by Carrier (1965) is used. Here the velocity in the nonlinear terms is replaced by the interior velocity multiplied by a modified Oseen parameter (m) which is later calculated in some meaningful manner. The case $m = 1$ is then the classical Oseen approximation.

The temperature calculations were first carried out for a step function input to region (a). When this solution was carried around until it was again input to this region the temperature was found to be more closely approximated by a bilinear profile: $\theta = \theta_1$, constant, out to $\xi = \xi_1$; $\theta = \theta_1 - \text{const.}\ (\xi - \xi_1)$ out to $\theta = 0$. Choice of this second profile gives a solution which satisfies the periodicity requirement. Equating the heat flux through a horizontal boundary to $2A$, i.e.

$$\int_0^L \frac{\partial\theta}{\partial\xi}(x,0)\,dx = 2A,$$

gives the following result:

$$H = \frac{A}{\omega_0^{\frac{1}{2}}} = \frac{1}{\pi^{\frac{1}{2}}}(1+\gamma)\left[x_1\left(\frac{B}{2}\right)^{\frac{1}{2}} + \mathscr{H}^{\frac{1}{2}}\left\{\left(L-\frac{3}{2}x\right)^{\frac{1}{2}} - \left(\frac{x_1}{2}\right)^{\frac{1}{2}}\right\}\right]$$

$$+\gamma\left[x_1\left(\frac{B}{2}\right)^{\frac{1}{2}}\frac{1}{\pi^{\frac{1}{2}}}\sum_0^\infty \frac{(-1)^n}{2n+1}y^{2n} - \frac{\beta}{2\omega_0^{\frac{1}{2}}}\left\{L-2x_1-4(L-2x_1)\right.\right.$$

$$\left.\left.\times i^2\operatorname{erfc}\left(\left(\frac{\mathscr{H}\omega_0}{4(L-2x_1)}\right)^{\frac{1}{2}}\frac{1}{\beta}\right)\right\}\right] + \left(1-\frac{\mathscr{H}\omega_0 x_1}{4A^2}\right)\frac{\mathscr{H}\omega_0 x_1}{4A}, \tag{20}$$

where $y = \left(\frac{B\omega_0\pi}{2}\right)^{\frac{1}{2}}\frac{\gamma}{A}x_1$,

$$\gamma = \theta_1 + \frac{1}{\xi_2}\left(\frac{4(1-2z_1)}{\alpha\omega_0}\right)^{\frac{1}{2}}\left\{i\operatorname{erfc}\left(\left(\frac{\alpha\omega_0}{4(1-2z_1)}\right)^{\frac{1}{2}}\xi_2\right) - i\operatorname{erfc}\left(\left(\frac{\alpha\omega_0}{4(1-2z_1)}\right)^{\frac{1}{2}}\xi_1\right)\right\},$$

$$\theta_1 = 1 - \left(\frac{B\omega_0}{2}\right)^{\frac{1}{2}}\frac{z_1}{A}\,i\operatorname{erfc}0,$$

$$\xi_1 = 2\frac{1-\theta_1}{\theta_1}\frac{A}{\alpha\omega_0}\frac{1}{2-\theta_1},$$

$$\xi_2 = 2\frac{1}{\theta_1}\frac{A}{\alpha\omega_0}\frac{1}{2-\theta_1},$$

$$\beta = \frac{\gamma}{2}\left[\frac{A}{B\omega_0 x_1} - \gamma\left(\frac{2}{B\omega_0}\right)^{\frac{1}{2}}\frac{1}{\pi^{\frac{1}{2}}}\{y^{-1}\arctan y - 1\}\right]^{-1}.$$

3.1. *The free case*

When all boundary conditions are free ($\nabla^2\psi = 0$ on all boundaries for rectangular geometry), $a = \frac{1}{3}$, and along each boundary there is a boundary layer of width $\sim R^{-\frac{1}{3}}$ in which $\theta \neq 0$ and the vorticity, $R^{\frac{2}{3}}\omega_0$ in the interior, decreases to zero. Since the velocities introduced by the boundary-layer streamfunctions are an

order of magnitude smaller than the interior velocities in the boundary layers, the classical Oseen approximation is exact to this order.

A linear profile is taken as input into region (*e*) and with suitable approximations the boundary-layer vorticity is followed round the cell until it is again input into region (*e*). These inputs are then matched and the periodicity relation obtained. Both the extent of this profile and a relation between A and w_0 are to be determined by this periodicity requirement. With the approximations used here only one relation is found and it is therefore assumed that the length scales of the temperature and vorticity variations in the vertical boundary layers are equal. The computations show that a factor of two change in the ratio of these lengths (j) introduces a variation of about 15 % in the Nusselt number.

The relation obtained is

$$\underbrace{\frac{A}{\alpha\omega_0^2}\left\{i^2\operatorname{erfc}0-\frac{1}{\sigma-1}\left[\sigma i^2\operatorname{erfc}\left(\frac{l_3}{\sqrt{\sigma Z}}\right)-i^2\operatorname{erfc}\left(\frac{l_3}{Z}\right)\right]\right\}}_{\text{(i)}}+\underbrace{\left(1+\frac{\gamma}{\theta_1}\right)\frac{1}{B\omega_0 Z^2}}_{\text{(ii)}}$$

$$=\underbrace{\frac{l_3}{l_2}\left\{i^2\operatorname{erfc}0-i^2\operatorname{erfc}\left(\frac{l_2}{\sqrt{\sigma Z}}\right)\right\}}_{\text{(iii)}}+\underbrace{\frac{l_3}{l}\frac{X}{Z}\frac{x_1}{z_1}\left\{i^2\operatorname{erfc}0-i^2\operatorname{erfc}\left(\frac{l}{\sqrt{\sigma X}}\right)\right\}}_{\text{(iv)}}$$

$$+\underbrace{\frac{x_1^2+z_1^2}{2B\omega_0 z_1 Z^2}\left\{\frac{l_3}{z_1 l_4}+\frac{l_3}{x_1 l_2}\right\}}_{\text{(v)}}, \tag{21}$$

where

$$X=\left(\frac{4(L-2x_1)}{\omega_0}\right)^{\frac{1}{2}}$$

$$Z=\left(\frac{4(1-2z_1)}{\omega_0}\right)^{\frac{1}{2}}$$

$$l_4=j\frac{A}{a\omega_0\gamma}\frac{2}{\sqrt{\pi}};$$

$j\sim 1$ is the ratio of the scales of the temperature and vorticity variations in the vertical boundary layers.

$$\omega_0\frac{l}{2}=\omega_0\frac{l_4}{2}\frac{z_1}{x_1}-\sigma\frac{\gamma}{\alpha\omega_0}\frac{z_1^2}{x_1}+\frac{\sigma}{2l_4 z_1\mathscr{H}}(z_1^2+x_1^2),$$

$$l_1=l+\frac{2}{l}X^2\sigma\left\{i^2\operatorname{erfc}0-i^2\operatorname{erfc}\left(\frac{l}{\sqrt{\sigma X}}\right)\right\},$$

$$\omega_0\frac{l_2}{2}=\frac{\omega_0}{2}\frac{l_1 x_1}{z_1}+\frac{\sigma}{2l_1 x_1\alpha}(x_1^2+z_1^2)-\frac{\sigma\theta_1}{\alpha\omega_0}z_1.$$

The terms in this balance may be identified as

(i) vorticity creation in the central vertical region, region (*a*);
(ii) creation in the other vertical regions (*h*) and (*b*);
(iii) conduction through the boundary of region (*a*);
(iv) conduction through the boundary of region (*e*);
(v) conduction through the boundaries of regions (*b*), (*d*), (*f*).

We thus have a balance between the creation of vorticity by the buoyancy and the conduction of vorticity through the boundaries.

Since $H = A/\sqrt{\omega_0}$ and $F = A/\omega_0^2$ defined in (20) and (21), have only a slight dependence on A and ω_0, an iterative procedure is used in the computations, $A = H^{\frac{4}{3}}/F^{\frac{1}{3}}$ and $\omega_0 = (H/F)^{\frac{1}{3}}$ being recalculated at the end of each iteration.

In this work the Rayleigh number is $R = g\alpha\Delta T d^3/\kappa\nu$ with a temperature difference of $2\Delta T$ between the plates. It is more usual to use the total temperature difference in the definition of the Rayleigh number, i.e. $R_1 = g\alpha 2\Delta T d^3/\kappa\nu$. The Nusselt number is $N = (A/L)R^{\frac{1}{3}} = 0{\cdot}79(A/L)R^{\frac{1}{3}}$ and, since it is the second proportionality constant, $0{\cdot}79A/L$, which must be compared with other work, it is this quantity which has been computed. The interior vorticity is similarly scaled using the Rayleigh number R_1.

The results of the calculations, together with values computed by Fromm (1965), are given in figure 3. In both curves the Nusselt number is a maximum

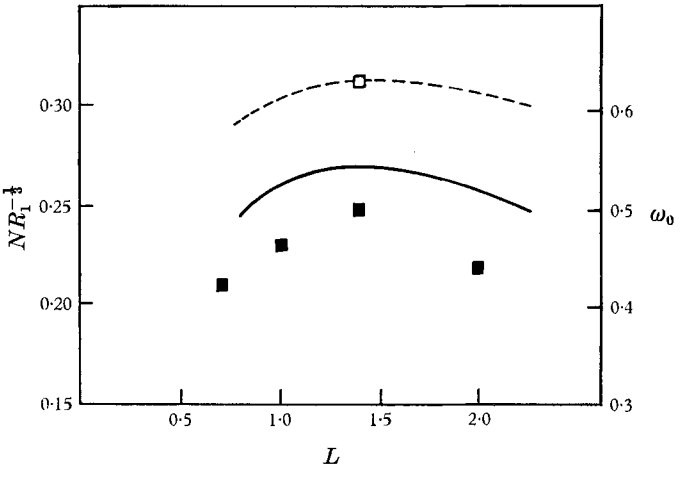

FIGURE 3. Free boundary conditions, $\sigma = 1$. —, scaled Nusselt number versus cell width; ■, Nusselt number values from Fromm (1965); – – –, scaled interior vorticity versus cell width; □, interior vorticity value from Fromm (1965).

for $L \approx 1{\cdot}4$; this maximum Nusselt number is $N \approx 0{\cdot}27R^{\frac{1}{3}}$ in the present work. The difference of 10 % between the results of the two theories is within the expected error (15 %) of this work. The values for the interior vorticities are also in good agreement. As shown in figure 4 there is very little dependence of the results on the Prandtl number.

The qualitative behaviour predicted by the theory is also in agreement with the computed results. In figure 6 of Fromm (1965) we find that (i) the vorticity is approximately constant in the interior; (ii) the boundary layers increase in width along the horizontal boundaries as vorticity is conducted through these boundaries and decrease in width along the vertical boundaries where both creation and conduction are important; (iii) the temperature in the interior is approximately zero and there is a sharp temperature gradient where the jets impinge

on the horizontal boundaries, and (iv) the widths of the temperature and vorticity boundary layers are comparable. Since the value of the Rayleigh number in this figure (12000) is not very large the boundary layers are still fairly wide.

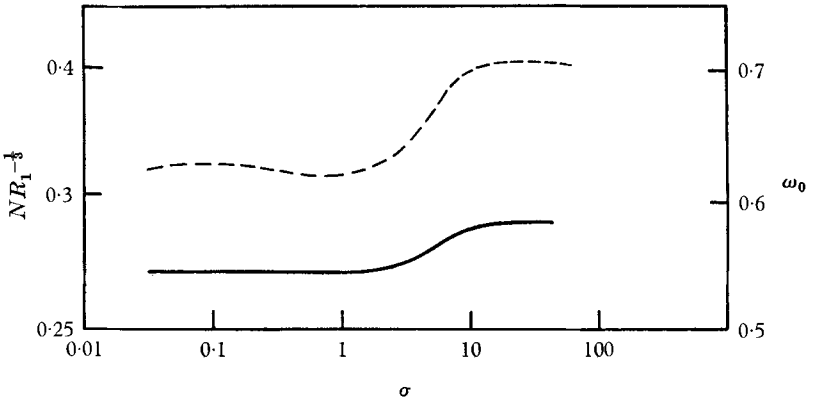

FIGURE 4. Free boundary conditions, $L = 1{\cdot}4$. —, scaled Nusselt number versus Prandtl number; – – –, scaled interior vorticity versus Prandtl number.

3.2. *The rigid case*

When all boundaries are rigid, $a = \frac{1}{4}$. All boundary-layer velocities are of the same order of magnitude as the interior velocities and the Oseen approximations are used. Since to highest order there is no net vorticity conduction across the horizontal boundaries, an estimate of the heat flux/vorticity relation is obtained using the vorticity conduction/creation balance in the vertical boundary layers.

In the vertical boundary layers the highest-order boundary-layer velocity equation is

$$\frac{1}{\sigma}\left\{\left(u_1+u_{BL}+\frac{\partial u_0}{\partial x}\xi\right)\frac{\partial v_{BL}}{\partial \xi}+v_{BL}\frac{\partial v_0}{\partial z}+(v_{BL}+v_0)\frac{\partial v_{BL}}{\partial z}\right\}=\frac{\partial^2 v_{BL}}{\partial \xi^2}+\theta,$$

with boundary conditions $v_{BL}+v_0 = 0$, $u_1+u_{BL} = 0$ on $\xi = 0$. On this boundary therefore

$$-\frac{1}{\sigma}\frac{1}{2}\frac{\partial}{\partial z}(v_0^2)=\frac{\partial^2 v_{BL}}{\partial \xi^2}+\theta.$$

The vorticity conduction across the boundary is

$$-\int_0^1 \frac{\partial \eta}{\partial \xi}(0,z)\,dz=\int_0^1 \theta(0,z)\,dz, \tag{22}$$

since $v_0(0) = v_0(1) = 0$. For the horizontal boundaries the buoyancy term does not appear to this order and the vorticity conduction across these boundaries is zero. A different proof of this result is given by Pillow (1952). The highest-order boundary-layer vorticity is here of order (interior velocity)/δ_{BL}. If vorticity of this order were convected round the corners (with $\delta_{\text{corner}} \gg \delta_{BL}$, as noted above) this would give rise to velocities of order (vorticity $\times\, \delta_{\text{corner}}$) $\gg$ interior velocity. The highest-order vorticity will therefore be restricted to the boundary layers along each side of the cell, a conclusion in agreement with the computed figures of Fromm (1965).

The right-hand side of (22) is found using the results of the temperature calculations. The left-hand side will be approximated by taking

$$\frac{\partial \eta}{\partial \xi} \approx \frac{v_0(z)}{L^2(z)};$$

and assuming that $L(z)$ may be closely approximated by the length scale of the temperature variations, i.e.

$$L^{(\mathrm{vort})}(z) \approx jL^{(\mathrm{temp})}(z), \quad j \sim 1.$$

This gives

$$-\int_0^1 \frac{v_0(z)}{L^2(z)}\,dz \approx j^2 \int_0^1 |\theta(0,z)|\,dz,$$

where $L(z)$ is now the length scale of the temperature variations.

The required relation is

$$\frac{\omega_0^3}{A^2}\left\{B^2 \frac{z_1}{16}(1+\pi\gamma^2) + a^3 \frac{\pi(1-2z_1)}{12}(\theta_1^2+\theta_1\gamma+\gamma^2)\right\}$$
$$= j^2\left\{z_1(1+\gamma) - \left(\frac{B\omega_0}{2}\right)^{\frac{1}{2}} \frac{i\,\mathrm{erfc}\,0}{A}\frac{z_1^2}{2} + \theta_1(1-2z_1)\right\}, \qquad (23)$$

where γ, θ, etc. are as previously defined.

An iterative procedure is again used in the computation. Since a rather crude approximation for $\partial\eta/\partial\xi$ ($\xi = 0$) has been used the results are expected to be accurate to only about 30 %.

The calculations have been carried out with a modified Oseen approximation. Since this problem has not been solved in any detail a reasonable value of the modified Oseen parameter, m, is chosen by comparison with the similar work of Weinbaum (1964) for rigid boundaries and cylindrical cross-section. His values are:

$$m = 0{\cdot}152,$$
$$\frac{(\omega_0)\text{ modified Oseen}}{(\omega_0)\text{ classical Oseen}} = 2{\cdot}57,$$
$$\frac{(N)\text{ modified Oseen}}{(N)\text{ classical Oseen}} = 0{\cdot}622 \quad \text{for} \quad \sigma = 1.$$

The results of the present work for $m = 0{\cdot}152$ and $L = 1{\cdot}5$ are

$$\frac{(\omega_0)\text{ modified Oseen}}{(\omega_0)\text{ classical Oseen}} = 2{\cdot}56,$$
$$\frac{(N)\text{ modified Oseen}}{(N)\text{ classical Oseen}} = 0{\cdot}625$$

(the present results are independent of σ).

Thus the modified Oseen results are independent of the choice of a criterion determining m from the three ratios given above.

The results given in figure 5 are

$N \approx 0{\cdot}63R^{\frac{1}{4}}$ (classical Oseen, maximum at $L \approx 2{\cdot}5$),

$N \approx 0{\cdot}59R^{\frac{1}{4}}$ (classical Oseen, $L \approx 1{\cdot}5$).

$N \approx 0{\cdot}37R^{\frac{1}{4}}$ (modified Oseen, $L \approx 1{\cdot}5$), with a possible error, apart from that due to the Oseen approximation, of about 30 %. J. E. Fromm has provided the author with a more detailed graph of his computed results than that given in his paper and the dependence $R \approx 0{\cdot}24R^{\frac{1}{4}}$ for rigid boundaries (two rolls within each enclosure) is taken from that graph.

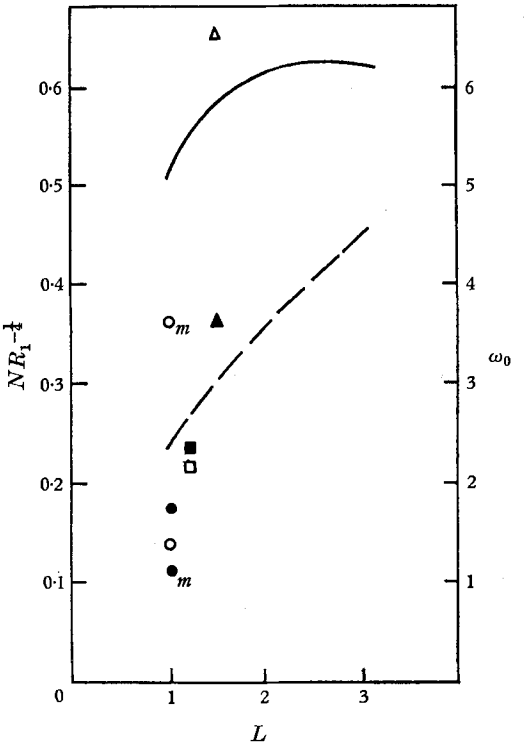

FIGURE 5. Rigid boundary conditions, $\sigma = 1$. —, scaled Nusselt number versus cell width; ▲, modified Oseen estimate of Nusselt number; ●, cylindrical geometry, classical Oseen estimate of Nusselt number (Weinbaum 1964); $\bullet_m$, cylinderical geometry, modified Oseen estimate of Nusselt number (Weinbaum 1964); ■, computed value of Nusselt number (Fromm 1965); – – –, scaled interior vorticity versus cell width; △, modified Oseen estimate of interior vorticity; ○, cylindrical geometry, classical Oseen estimate of interior vorticity (Weinbaum 1964); O_m, cylindrical geometry, modified Oseen estimate of interior vorticity (Weinbaum 1964); □, computed value of interior vorticity (Fromm 1965).

It appears likely that much of the difference between these results is due to the use of the Oseen approximations; it must be noted that the modified Oseen result is a decided improvement over the classical Oseen result. The heat flux

$$-\int_0^L \frac{\partial \theta}{\partial \zeta}(\zeta = 0)\,dx$$

is a local quantity in the horizontal boundary layers, being calculated at the boundary rather than averaged over the entire boundary-layer region, and it is suggested that this may explain the large errors.

The qualitative behaviour predicted by the present work may be compared with figure 10 of Fromm (1965). Since there are two convection cells within the rigid boundaries this figure contains features of both the periodic rigid and rigid boundary condition cases.

The temperature profile is similar to those for the free boundary conditions. Along each rigid boundary is a concentration of vorticity; each vorticity concentration is restricted to the particular boundary-layer region, for both horizontal and vertical boundaries. The length scales of the vorticity and temperature variations in the vertical boundary layers are comparable.

3.3. *Periodic rigid boundaries*

In the case of periodic rigid boundaries the horizontal boundaries are rigid and the vertical boundaries are free (the boundary conditions for motion periodic in the horizontal direction; see Fromm (1965)). Thus $a = \frac{1}{3}$, and the Oseen approximations are used in the horizontal boundary layers.

The rigid horizontal boundaries introduce a vorticity of order R^1, whereas the interior vorticity is of order $R^{\frac{2}{3}}$. However as in the rigid case the net vorticity conducted across each horizontal boundary is zero and this large vorticity is confined to these regions.

As in the free case there must be a balance between vorticity creation and conduction in each cell: that is, there must exist a periodic vorticity boundary-layer solution of order $R^{\frac{2}{3}}$. The vorticity conduction across the horizontal boundaries is now a second-order effect but may be calculated from the first-order solution.

If the asymptotic expansion for the velocity is

$$\mathbf{v} = R^{\frac{2}{3}}\mathbf{v}_0 + R^{\frac{1}{3}}\mathbf{v}_1 + \mathbf{v}_2 + \ldots + R^{\frac{2}{3}}\mathbf{v}_{BL} + R^{\frac{1}{3}}\mathbf{v}'_{BL} + \ldots,$$

then the second-order velocity boundary-layer equation on a rigid boundary is

$$\frac{1}{\sigma}\left\{(u_0+u_{BL})\frac{\partial u_{BL}}{\partial x} + u'_{BL}\frac{\partial}{\partial x}(u_0+u_{BL}) + \left(\frac{\partial v_0}{\partial z} + v_{BL} + v_1\right)\frac{\partial^2 u_{BL}}{\partial \zeta} + u_1\frac{\partial u_{BL}}{\partial x} + u_{BL}\frac{\partial u_1}{\partial x} + v_{BL}\frac{\partial u_0}{\partial z} + (v_2+v_{BL})\frac{\partial u_{BL}}{\partial \zeta}\right\} = \frac{\partial^2 u'_{BL}}{\partial \zeta^2}, \tag{24}$$

with boundary conditions

$$u_0 + u_{BL} = 0, \qquad v_1 + v_{BL} = 0,$$
$$u_1 + u'_{BL} = 0, \qquad v_2 + v'_{BL} = 0 \quad \text{on} \quad \zeta = 0.$$

Using these boundary conditions the equation becomes on this boundary

$$\frac{\partial \eta'_{BL}}{\partial \zeta}(x,0) = \frac{\partial^2 u_{BL}}{\partial \zeta^2}(x,0) = \left[\frac{\partial}{\partial x}(u_{BL}u_1) + v_{BL}\frac{\partial u_0}{\partial \zeta}\right]\frac{1}{\sigma}.$$

Now $\partial u_0/\partial z = -\omega_0$ on this boundary and $u_{BL}u_1 = 0$ for $x = 0, L$. The net second-order vorticity conduction across this horizontal boundary is thus

$$\int_0^L \frac{\partial \eta^1}{\partial \zeta}(x,0)\,dx = -\frac{\omega_0}{\sigma}\Big[\psi_{BL}(\zeta=0)\Big]_0^L. \tag{25}$$

Using this result the requirement that a periodic vorticity boundary layer should exist gives the following equation:

$$\underbrace{\frac{A}{\alpha\omega_0^2}\left\{i^2\operatorname{erfc}0-\frac{1}{\sigma-1}\left(\sigma i^2\operatorname{erfc}\left[\frac{l_3}{\sigma^{\frac{1}{2}}Z}\right]-i^2\operatorname{erfc}\left[\frac{l_3}{Z}\right]\right)\right.}_{\text{(i)}}+\underbrace{\left.\left(1+\frac{\gamma}{\theta_1}\right)\frac{1}{B\omega_0 Z^2}\right\}}_{\text{(ii)}}$$

$$=\underbrace{\frac{l_3}{l_2}\left\{i^2\operatorname{erfc}0-i^2\operatorname{erfc}\left[\frac{l_2}{\sigma^{\frac{1}{2}}Z}\right]\right\}}_{\text{(iii)}}+\underbrace{\frac{1}{2B\omega_0 Z^2}\left\{\frac{l_3}{l_4}+\frac{l_3}{ml_1}\frac{z_1}{x_1}\right\}}_{\text{(iv)}}$$

$$+\underbrace{\frac{1}{(\sigma\omega_0)^{\frac{1}{2}}}\frac{1}{\mathscr{H}Z^2}\frac{x_1}{z_1}\frac{l_3}{m^{\frac{1}{2}}}\left\{(2B)^{\frac{1}{2}}x_1\,0{\cdot}443+\mathscr{H}^{\frac{1}{2}}\,1{\cdot}128((L-x_1-x')^{\frac{1}{2}}-(x_1-x')^{\frac{1}{2}})\right\}}_{\text{(v)}}, \tag{26}$$

where x_1, z_1, X, Z, θ, l_4 are as defined previously and

$$l=l_4\frac{z_1}{x_1}+\frac{\sigma}{\alpha\omega_0^2}\frac{z_1^2}{x_1}\left(\frac{1}{l_4}-2\gamma\right),$$

$$m\frac{\mathscr{H}\omega_0^2}{2}(l_1-l)=\omega_0\left\{\left(\frac{2B\omega_0\sigma}{m}\right)^{\frac{1}{2}}x_1\frac{i^2\operatorname{erfc}0}{i\operatorname{erfc}0}+\left(\frac{\mathscr{H}\omega_0\sigma}{m}\right)^{\frac{1}{2}}\right.$$
$$\left.\times\,1{\cdot}128((L-x_1-x')^{\frac{1}{2}}-(x_1-x')^{\frac{1}{2}})\right\},$$

$$\frac{\omega_0}{2}l_2=\frac{m\omega_0}{2}l_1\frac{x_1}{z_1}+\frac{\sigma}{2ml_1x_1\alpha}z_1^2-\frac{\sigma\theta_1}{\alpha\omega_0}z_1,$$

$$x'=0{\cdot}695x_1.$$

As in the free case the terms in this balance may be identified as:

(i) vorticity creation in the central vertical region, region (*a*);

(ii) creation in the other vertical regions, (*h*) and (*b*);

(iii) conduction through the boundary of region (*a*);

(iv) conduction through the boundary of regions (*h*), (*b*);

(v) conduction through the horizontal boundary regions (*d*), (*e*).

One scheme for determining the modified Oseen parameter m is to substitute our approximate solutions in one of the nonlinear equations governing the flow in the boundary layers and to require that the integrated average of this over all boundary-layer space be zero. However, foı both the velocity and the temperature equations, the m-dependence cancels out when the integration is performed. A more satisfactory method would be to minimize the integral over this space of the square of the function I defined below; that is to minimize

$$\int\int I^2 d\zeta dx.$$

Since this calculation involves a total of 25 terms it was decided to minimize the quantity

$$\int_0^L\left[\int_0^\infty I^2 d\zeta\right]^2 dx;$$

it is not expected that the values for m obtained from these two methods should differ by much.

The function $I(x, \zeta)$ is defined by substituting the approximate solutions in the horizontal boundary-layer velocity equation; i.e.

$$I(x,\zeta) = \frac{1}{\sigma}\left\{(u_0+u_{BL})\frac{\partial u_{BL}}{\partial x}+u_{BL}\frac{\partial u_0}{\partial x}+\left(\frac{\partial v_0}{\partial z}\zeta+v_{BL}+v_1\right)\frac{\partial u_{BL}}{\partial \zeta}\right\}-\frac{\partial^2 u_{BL}}{\partial \zeta^2}.$$

The results are shown in figures 6, 8. The Nusselt number is $N = 0{\cdot}24R^{\frac{1}{3}}$ (classical Oseen), $N = 0{\cdot}15R^{\frac{1}{3}}$ (modified Oseen), being a maximum for $L = 1{\cdot}4$. The expected error in this estimate, apart from that due to the Oseen approximations, is about 15 %.

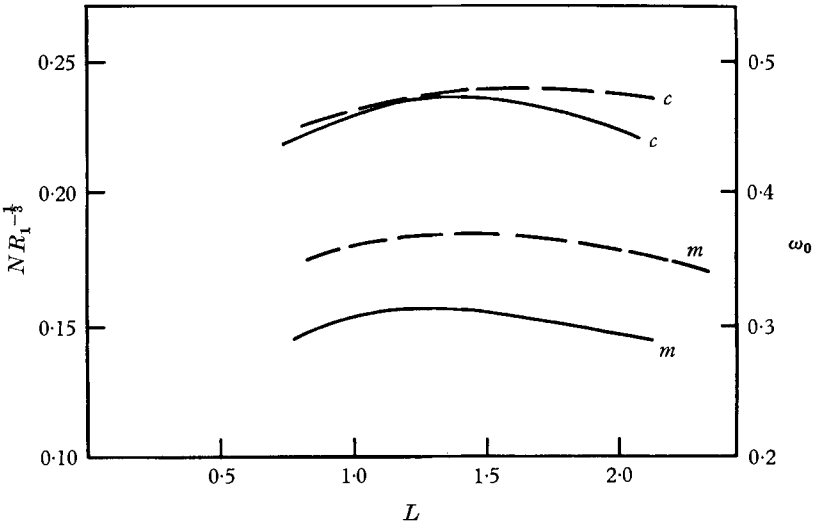

FIGURE 6. Periodic rigid boundary conditions, $\sigma = 1$. —, scaled Nusselt number; – – – scaled interior vorticity; *c*, classical Oseen estimate; *m*, modified Oseen estimate.

For very large Rayleigh number and therefore turbulent motion the available experimental data may be fitted by $N = 0{\cdot}085R^{\frac{1}{3}}$. It may be reasonably argued that the heat flux for the laminar flow will give a lower bound to the heat flux for turbulent motion, which would indicate that the modified Oseen result is at least 60 % too large. This error is similar to that found in the calculations for the rigid case and it is suggested that these large errors are due to the use of the Oseen approximations (once again the modified Oseen result is a considerable improvement over the classical Oseen result).

The $\frac{1}{3}$-power law dependence of the Nusselt number on the Rayleigh number predicted here is not followed by the results of Fromm's computations, which may be fitted by $N \approx 0{\cdot}19R^{0{\cdot}28}$. An explanation of this difference may be given as follows.

The heat flux for free vertical boundaries is expected to be greater than that for rigid boundaries and this is indeed so for large enough Rayleigh number. However for $R = 4 \times 10^5$ we have $0{\cdot}24R^{\frac{1}{3}} = 0{\cdot}085R^{\frac{1}{3}}$ and below this value the flux

predicted for the rigid boundaries is greater than that predicted for periodic vertical boundaries. It is suggested that the flow adjusts itself so as to give the maximum possible heat flux, and that a velocity variation will appear beside the vertical boundaries for $R < 4 \times 10^5$. The heat flux calculated for the rigid boundaries will be a lower bound for this flow as in that case the velocities on the vertical boundaries were taken to be zero.

In figure 7 the computed results (Fromm 1965) for the periodic rigid case are given together with the computed curve $N = 0{\cdot}24R^{\frac{1}{4}}$ for the rigid case and a

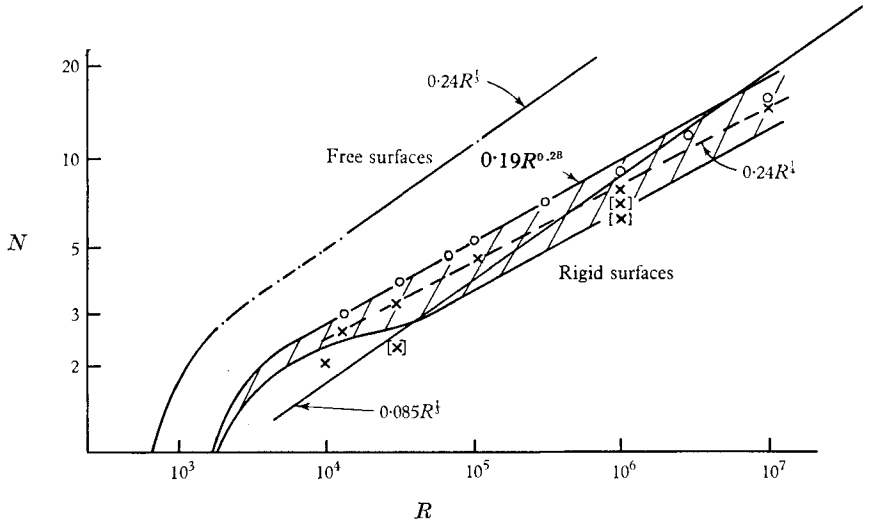

FIGURE 7. Computed results, Fromm (1965). ○, cyclic vertical boundaries; ×, rigid vertical boundaries.

$\frac{1}{3}$-power curve $N = 0{\cdot}085R^{\frac{1}{3}}$; the constant being adjusted to fit the experimental results at high Rayleigh number (the drop-off of the periodic rigid results above $R = 3 \times 10^5$ is thought to relate to insufficient resolution of the boundary layer (Fromm, private communication)). The Nusselt number for the periodic rigid case is seen to vary in the predicted manner and this also agrees well with the experimental results.

Thus the model suggested by Pillow following the assumption that the buoyancy torque is balanced by the shear stress on the horizontal boundaries (equivalent to the assumption of velocity boundary layers in the vertical) is consistent with observations for $R_{\text{crit}} \ll R < 4 \times 10^5$, and the model presented here, which assumes only those boundary layers necessary to satisfy the boundary conditions, is valid for $R > 4 \times 10^5$.

The dependence of the Nusselt number and the interior vorticity on the Prandtl number σ is shown in figure 8, together with three experimental values of the Nusselt number (Rossby 1966) scaled to the classical Oseen theoretical value at $\sigma = 6{\cdot}8$.

The qualitative picture agrees well with the computations of Fromm (1965) below $R \sim 3 \times 10^5$ at which Rayleigh number some time dependence appears in the computed results.

4. Turbulence

Let us assume that turbulence or time dependence will occur when some boundary layer becomes unstable.

Notation: boundary-layer Rayleigh number $R_\delta = R(\delta/d)^3$; boundary-layer Reynolds number $Re = u'_{BL}\delta/\nu$, where u'_{BL} is the dimensional boundary-layer velocity, δ is the dimensional boundary-layer width.

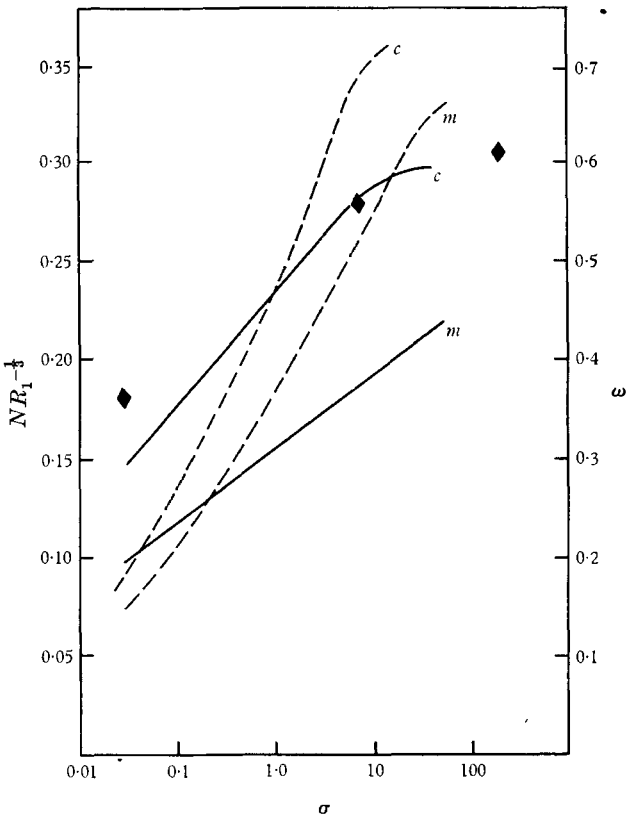

FIGURE 8. Periodic rigid boundary conditions, $L = 1{\cdot}4$. —, scaled Nusselt number versus Prandtl number; – – –, scaled interior vorticity versus Prandtl number; *c*, classical Oseen estimate; *m*, modified Oseen estimate; ◆, scaled experimental Nusselt number (Rosby 1966).

In the free case both R_δ, Re are independent of the Rayleigh number R in all boundary layers and there is no indication of possible instability.

For periodic rigid boundary conditions we have in the horizontal boundary layers $\delta \sim \sigma^{\frac{1}{2}}R^{-\frac{1}{3}}d$ and $u'_{BL} \sim R^2\kappa/d$, giving $Re \sim R^{\frac{1}{3}}/\sigma^{\frac{1}{2}}$. There is thus a possibility of shear flow instability in the horizontal boundary layers. If turbulence occurs for a particular Reynolds number, then $R_T \sim \sigma^{\frac{3}{2}}$, where R_T is the critical Rayleigh number for onset of turbulence. The boundary-layer Reynolds numbers in the vertical boundaries and all the boundary-layer Rayleigh numbers are independent of R and there is thus no indication of any other instability.

We note the following two qualitative features of such a breakdown mechanism. They are: (i) the instabilities occur within the horizontal boundary layers and (ii) the vertical jets are stable.

In the rigid case $R_\delta \sim R^{\frac{1}{4}}$, $Re \sim R^{\frac{1}{2}}$ in all boundary layers and both types of instability are possible.

This work suggests the following quasi-steady model of turbulent convection. Each cell is steady until an instability in a horizontal boundary layer causes a new vertical jet to form (these jets forming in a random manner). If within this jet it is required that balances between the vorticity creation, conduction and convection and heat conduction and convection hold, we obtain a $\frac{1}{3}$-power Rayleigh number dependence for the Nusselt number as for free vertical boundaries of a steady convection cell.

As long as for the major part of the time the motion is approximately steady the Nusselt number estimates for the steady cells will give an indication of the heat flux expected for turbulent motion.

However, the Prandtl number dependence of the critical Rayleigh number for this breakdown does not agree well with the available experimental data and perhaps a different instability mechanism is involved.

This may be compared with the similar model suggested by Howard (1965); in that work the $R^{\frac{1}{3}}$ Nusselt number dependence was obtained from the assumption that the heat flux at high Rayleigh number is independent of the separation of the plates.

A set of equations frequently used in the study of turbulence are the mean field equations. These are obtained by averaging over the horizontal and neglecting the 'fluctuating self-interaction' temperature convection terms. Neglect of the momentum convection terms may be considered to be appropriate for large Prandtl number ($\sigma \to \infty$) or may be justified by physical arguments (see, for example, Malkus (1956), Herring (1963)).

It has been conjectured that the heat flux predicted using the mean field equations maximizes the possible heat flux for the full Boussinesq equations (arguing that the neglected terms act only to reduce the heat flux). However Stewartson (1965), using these equations, has obtained a $c_1 R^{0\cdot3}[\log(c_2 R^{\frac{3}{2}})]^{-\frac{1}{5}}$ dependence of the maximum heat flux for one horizontal wave-number ($a = \lambda R^{\frac{1}{4}}$, $\lambda < 1$), which for high enough Rayleigh number will be less than the flux predicted by the $R^{\frac{1}{3}}$ power law suggested here and by Howard (1965).

If the momentum convection term is neglected velocity boundary layers (i.e. shear layers) near the horizontal rigid boundaries are not possible and it is suggested that the heat conducted through these boundaries may not be convected away as efficiently as it would be if such boundary layers were in existence (this point has been discussed by Kraichnan (1962) when considering a mixing length theory at turbulent convection). In fact the present model of steady convection cells breaks down if we take the limit $\sigma \to \infty$. The boundary layer considered by Stewartson is a thermal boundary layer.

We therefore find that for steady convection there will be more heat flux possible if the limiting process $R \to \infty$, for large σ, is used than if the limiting process is $\sigma \to \infty$ followed by $R \to \infty$ (even if the neglect of the momentum con-

vection terms is justified by physical arguments it remains mathematically equivalent to taking the limit $\sigma \to \infty$ for steady, or statistically steady, motions).

For the cellular motion studied in the present paper the difference between the cases 'σ large' and '$\sigma \to \infty$' is to be found by a comparison of the vorticity convection and conduction in the interior; i.e. which is the largest, $\sigma^{-1}J(\psi, \nabla^2\psi)$ or $\nabla^4\psi$? For periodic rigid boundary conditions $\psi \sim R^{\frac{2}{3}}$ and therefore the criterion for small Prandtl number is that $\sigma \ll R^{\frac{2}{3}}$, and for large enough Rayleigh numbers this will be true for all physical Prandtl numbers. It is uncertain whether the dividing criterion for σ large/small should be $\sigma \sim R^{\frac{2}{3}}$ or $\sigma \sim (R/R_{\text{crit}})^{\frac{2}{3}}$. If it is in fact the latter then results obtained using the mean field equations will be valid for many real problems (σ large and moderate R/R_{crit}).

5. Laminar free convection in a vertical slot

In a recent paper, Gill (1966) considers the problem of the steady motion of a fluid between two vertical plates which are maintained at different temperatures such that the Rayleigh number of the problem is large. A model is postulated which seems to be in contradiction to that suggested by Batchelor (1954), and in good agreement with the available experimental data. Gill states that no reason seems to have been found for rejecting the Batchelor model on theoretical grounds. We present here a physical argument by which Gill's model may be derived from that of Batchelor.

The Batchelor model has been derived above and predicts a constant temperature and constant vorticity in the interior; Gill's model predicts a stratified interior temperature and an interior velocity smaller in order of magnitude than the boundary-layer velocity.

It has been shown by Weinbaum (1964) that, for a circular cross-section cellular motion with rigid boundaries and side-to-side heating the interior vorticity, ω_0, is zero.

The physical mechanism giving rise to this zero interior motion may be described with the aid of figure 9 which has been drawn following the assumption that the interior vorticity is non-zero. In regions a for both geometries the buoyancy forces are opposing the motion. If the viscous stresses acting on these regions are not sufficient to overcome the buoyancy forces the fluid there will slow down and the temperature difference, $T - T_0$, between these regions and the interior will gradually extend into the interior. Eventually when the interior motion has, to the highest order of magnitude, been reduced to zero by this mechanism the constant interior temperature will be replaced by a stable stratification.

Weinbaum has shown that this does occur for circular geometry in the Oseen approximation; the assumption made here is that the physical mechanisms are the same for both geometries (as illustrated in figure 9) and that the interior vorticity will be zero in the Batchelor model for rectangular geometry as it is for circular geometry.

Let us now re-examine the interior flow, noting that the streamlines for the most important interior motion ($R^{\frac{1}{4}}\mathbf{v}_1$) are not now closed, and that the proof that $\theta \equiv 0$ in the interior is no longer valid. The largest term in order of magnitude

in the vorticity equation is now $R\theta_x$ and therefore $(\theta_0)_x = 0$. The highest-order interior temperature equation is now $(\mathbf{v}_1 . \nabla)\theta_0 = 0$ and using the above result we obtain $(\mathbf{v}_1 . \hat{k}) = 0$ (provided $\theta_0 \neq 0$).

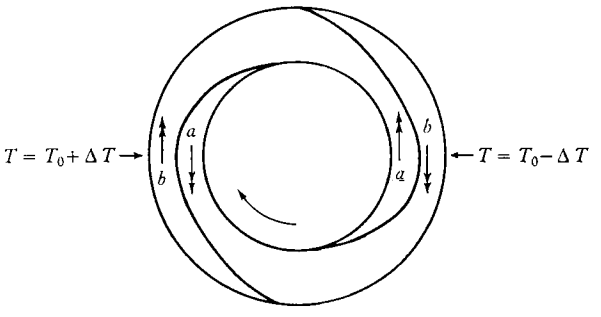

(*a*)

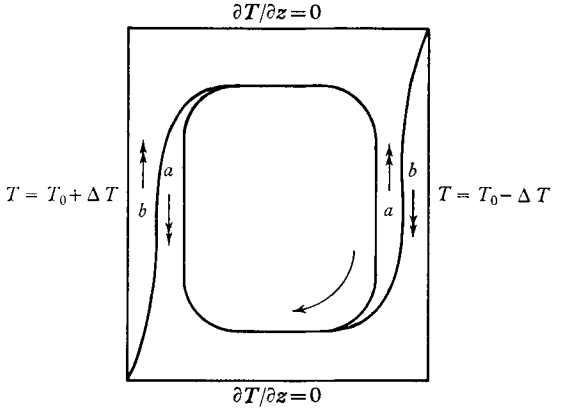

(*b*)

FIGURE 9. Cellular motion for side–side heating following the assumption that the highest-order interior velocity, $R^{\frac{1}{2}}v_0$, is non-zero. (*a*) Circular geometry. On the circumference $T = T_0 - \Delta T \cos\theta$, where θ is measured from the horizontal. (*b*) Rectangular geometry. —, isotherms, $T = T_0$; →, direction of core rotation; →→, direction of local buoyancy force.

We have thus, in a consistent manner, and with the introduction of Batchelor's model as a necessary step, arrived at Gill's model for this flow, with a boundary-layer velocity greater in order of magnitude than the interior velocity and a non-zero interior temperature which is independent of the horizontal co-ordinate.

The fact that the interior velocity is smaller in order of magnitude than the boundary-layer velocities allowed Gill to ignore the horizontal boundaries to a first approximation.

For unit Prandtl number this flow is equivalent to that between two rotating horizontal flat plates provided that

$$\frac{d}{r} \ll \frac{\delta\Omega}{\Omega} \ll 1 \quad \text{and} \quad T \gg 1, \quad \text{where} \quad T = \frac{2\Omega\,\delta\Omega r d^3}{\nu^2},$$

the Taylor number, is equivalent to the Rayleigh number; d is the separation of the plates; r is the mean radius of the region considered; Ω is the mean angular velocity; and $\delta\Omega$ is the difference of angular velocity between the two plates,

that is within a region at a large radius ($r/d \gg 1$) and of radial extent of the order of magnitude of the separation of the plates.

Although not all these criteria are satisfied, two features of flow between rotating plates as discussed in the literature (see for example Rogers & Lance 1964; Stewartson 1953) agree with the above model. These are the existence of boundary layers in the horizontal velocities near the plates with a rotational velocity in the interior which is intermediate between that of the two disks and a non-zero vertical interior velocity carrying fluid from one plate to the other.

It has been noted by Robinson (1965) that the interior flow for a simple model of the wind-driven ocean is not determined by the satisfaction of the inviscid boundary conditions, as is also the case in the problem considered here.

The author wishes to acknowledge the guidance, assistance and inspiration of his thesis adviser Prof. L. N. Howard under whose supervision this work was conducted.

The material in this paper is based on the author's Ph.D. thesis which was submitted to the Department of Mathematics at the Massachusetts Institute of Technology, Cambridge, Mass., and was further developed while the author was at the Institute of Geophysics and Planetary Physics, U.C.L.A., California, that work being sponsored by NSF grant GP-2414. Much of the work was developed while the author was a summer fellow at the Woods Hole Oceanographic Institute, Mass., in 1965, and appears in the Student Lectures of that year. The computations were performed at project MAC and the computation centre, M.I.T.

REFERENCES

BATCHELOR, G. K. 1954 *Quart. Appl. Math.* **12**, 209.

BATCHELOR, G. K. 1956 *J. Fluid Mech.* **1**, 177.

CARRIER, G. F. 1965 *J. Soc. Indust. Appl. Math.* **13**, 68.

CHANDRASEKHAR, S. 1961 *Hydrodynamic and Hydromagnetic Stability*. Oxford University Press.

FROMM, J. E. 1965 *Phys. Fluids* **8**, 1757.

GILL, A. 1966 *J. Fluid Mech.* **26**, 515.

HERRING, J. R. 1963 *J. Atmos. Sci.* **20**, 325.

HOWARD, L. N. 1965 *Proc. 11th Int. Cong. Appl. Mech.*

KRAICHNAN, R. H. 1962 *Phys. Fluids*, **5**, 1374.

MALKUS, W. V. R. 1956 *J. Fluid Mech.* **1**, 521.

PILLOW, A. F. 1952 *Aust. Dep. Supply Aero. Res. Lab. Rept.* A 79.

ROBINSON, A. 1965 *Research Frontiers in Fluid Dynamics*, p. 504 (ed. R. J. Seeger and G. Temple). Interscience Publishers.

ROGERS, M. H. & LANCE, G. N. 1964 *Quart. J. Mech. Appl. Math.* **17**, 319.

ROSSBY, H. T. 1966 *Sci. Rept. of the Geophys. Fluid Dyn. Lab., M.I.T.* no. 27.

SEGEL, L. A. 1966 *Non-equilibrium Thermodynamics, Variational Techniques, and Stability*, pp. 165–97. University of Chicago.

STEWARTSON, K. 1953 *Proc. Camb. Phil. Soc.* **49**, 333.

STEWARTSON, K. 1965 *Non-equilibrium Thermodynamics*, p. 158 (ed. R. J. Donnelly, R. Herman and J. Prigogine). University of Chicago Press.

WEINBAUM, S. 1964 *J. Fluid Mech.* **18**, 409.